VisAGGE: Visible Angle Grid for Glass Environments *

LIDAR mapping for glass, metal, mirrors, and other non-diffuse surfaces.

Paul Foster, Zhenghong Sun, Jong Jin Park, and Benjamin Kuipers[1]

***Abstract*— We describe a new algorithm for occupancy grid mapping using LIDAR in the presence of glass and other non-diffuse surfaces. This is a major problem for robot navigation in many indoor environments due to the prevalence of glass paned doors, windows, and even glass walls, as well as mirrors and polished metal surfaces. Current formulations of occupancy grid mapping make the assumption that objects in the environment are detectable from all angles. However, glass and other specular surfaces are invisible to LIDAR at most angles and so become washed out as "noise". We modify the standard occupancy grid algorithm to allow for mapping objects that are only visible from certain view angles, by tracking the subset of angles from which objects are reliably visible. We show that these angles can be determined reliably with a single pass through the environment, and that the information can be used to map both diffuse and specular surfaces.**

I. INTRODUCTION

Occupancy grid mapping is one of the most common methods of LIDAR mapping currently in use. By dividing the world into a uniform grid of cells and solving the mapping problem locally at each cell, occupancy grid mapping provides a representation of the environment that is general, robust, and easy to manipulate [1]. Occupancy grid maps are also inherently suitable for online mobile robot applications. Common uses for occupancy grid mapping include localization, path planning, and detection of motion.

Modern environments – like the one shown in Figure 1 – commonly contain glass architectural features such as glass paned doors, full height windows, glass dividers and so forth. Unfortunately, current implementations of occupancy grid maps tend to delete glass obstacles, as shown in Figure 2(a).

We show that the problem is caused by an overly simplistic model of the world and sensor that only accounts for diffuse objects. Our algorithm corrects this by substituting a more general model that takes into account the visibility of glass from different angles. At most angles, glass is transparent to LIDAR, or reflects the laser away from the sensor, creating spurious readings. The key insight to the algorithm is that – from the perspective of LIDAR – glass behaves like a diffuse object at some view angles, while from other angles it appears like free space. By learning these angles and only using LIDAR readings that are consistent with diffuse object behavior, we convert the problem of mapping glass back into the problem of mapping diffuse objects. Although our focus is on glass, the method applies equally well to mirrors, metal, and most other non-diffuse solids.

Our algorithm consists of a simple online heuristic for discovering a subset of the diffuse-like angles, and a method for reconstructing the observations from these angles in the presence of localization error. The latter is necessary because the diffuse-like angles often span a $< 2^\circ$ range around the surface normal, which is less than the uncertainty in the view angle at short range.

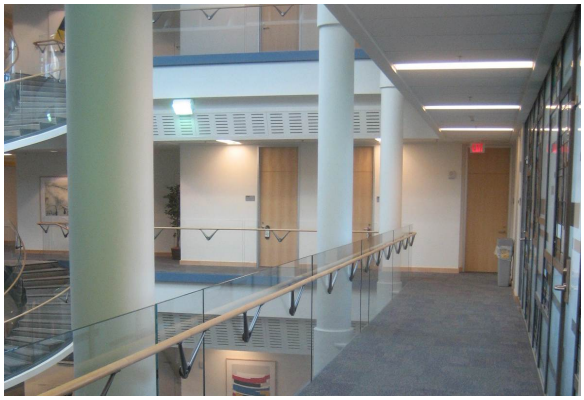

Fig. 1. Many modern built environments include highly transparent glass obstacles that are difficult for robot mapping methods to see. The maps presented in Figure 2 are of the environment shown, which includes both straight and curved glass walls.

II. PRIOR WORK

Previous work has attempted to address the problem of mapping glass with LIDAR by using sensor fusion, by modeling the probability of receiving direct reflections back from glass, using mirror symmetry of reflections, or analyzing the surrounding environment. This work has suffered from major problems with reliability, precision, and generality.

Diosi and Kleeman [2] attempt to get around the problem by using sonar to detect glass. This causes an unnecessary loss of precision in location and shape of the glass. Awais [3] attempted to model the probability of receiving a direct reflection back from the glass as a function of angle and distance. This is similar to our approach, but Awais makes the assumption that this function is gaussian, and the same for all pieces of glass, leading to gross errors in the detection of glass. Yang and Wang [4] attempt to take advantage of mirror-like reflections and locate glass by detecting the mirror symmetry of these reflections. However, detecting this

This work has taken place in the Intelligent Robotics Lab in the Computer Science and Engineering Division of the University of Michigan. Research of the Intelligent Robotics lab is supported in part by grants from the National Science Foundation (CPS-0931474, IIS-1111494, and IIS-1252987), and from the TEMA-Toyota Technical Center.

[1]PF, ZS, and BK are with the Computer Science & Engineering Division of the EECS Department, and JJP is with the Mechanical Engineering Department, all at the University of Michigan, Ann Arbor, MI 48109.
Email addresses: {pfost, zhsun, jongjinp, kuipers}@umich.edu.

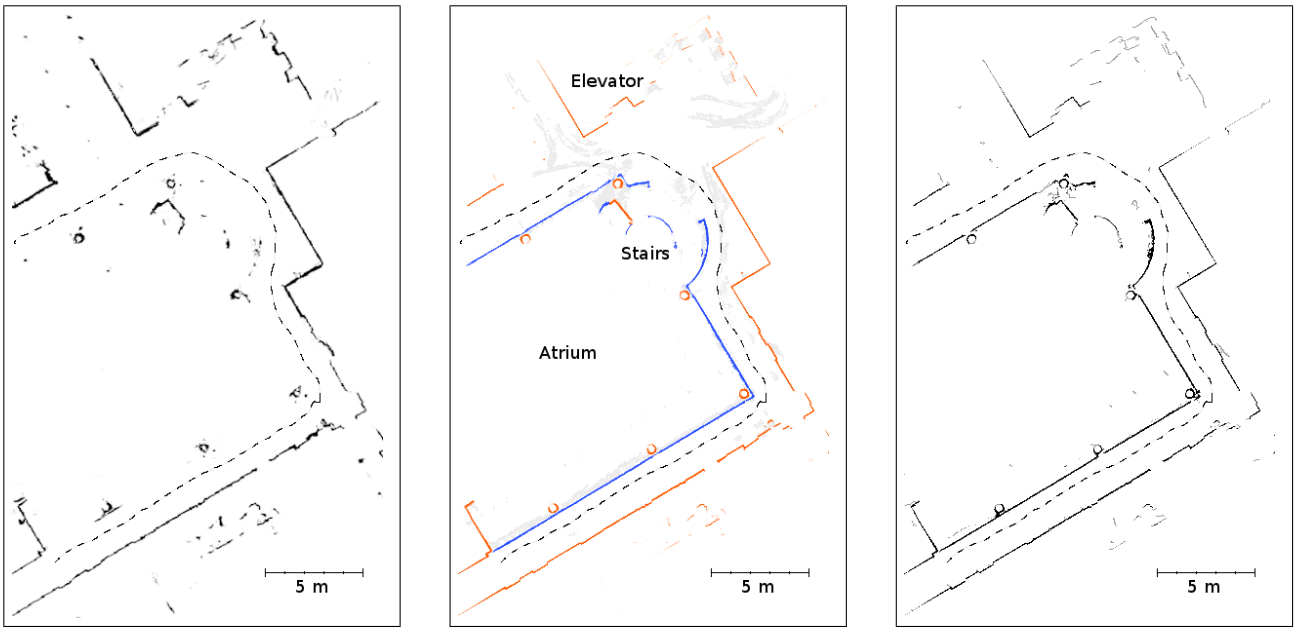

(a) Traditional occupancy grid mapping of the environment in Figure 1 (LIDAR sensor path shown as dashed line) produces a map in which most of the highly transparent glass walls are entirely missing, giving the illusion of navigable free space across the atrium. (Only 13% are correctly detected, mostly small regions of glass near the spiral staircase, which are visible due to subtle optical effects, refer to Section III-A.2). The shiny metal doors of the elevator are also missing, showing that the problem is general to other non-diffuse materials as well.

(b) Hand labeling the observations as glass walls (blue), diffuse walls(orange) and motion/reflection/noise(gray) shows that the glass information was available from the LIDAR, but was discarded. Three pedestrians traveling through the area are also visible as streaks of motion. There are also several complex reflections, which appear as clouds beyond the glass. Ideally, an occupancy grid map should be able to preserve the glass wall information while rejecting the observations caused by motion, reflections and noise.

(c) Using our algorithm, we preserve almost all of the glass walls (94%) while still eliminating nearly all of the unwanted cells. 99% of the glass detected is also correctly localized to within 1 cell (5 cm). The only missing segments are small pieces of glass near the pillars which are removed by our motion removal heuristic for the first pass through the environment.(Cells are not colored because our algorithm does not categorize materials into discrete glass and diffuse categories, instead modeling them as a continuum based on angles at which they are visible.)

Fig. 2. Maps of the environment in Figure 1. (5 cm cell size.)

symmetry is computationally challenging for flat surfaces and nearly intractable for curved surfaces. Another approach, seen for example in Pu and Vosselman [5], is to infer glass by detecting things like window frames, but this approach is limited to the model of the surroundings.

There has also been work on segmenting glass once mapped, as in Tatoglu and Pochiraju [6], but it did not address the problems of mapping glass in the first place.

In contrast to the above, our method directly locates glass with high precision using only LIDAR information, including the case of curved surfaces.

III. PHYSICS AND SENSOR MODELS

Before discussing how our algorithm deals with glass, we need to review how a LIDAR works and the behavior of a LIDAR in the presence of glass.

A LIDAR works by sending out pulses of laser light and then waiting for the light to come back. By measuring the time between sending and receiving the pulse, the LIDAR measures the distance to the target. [1] In this sense, LIDAR behaves very much like sonar. If the light doesn't come back, no distance is measured.

A. Physics Background

1) Light and Glass: As shown in Figure 3, when light hits a diffuse surface, it scatters equally in all directions, traveling outward in a hemispherical region. Because the power is distributed over the hemisphere, the power per unit solid angle is greatly reduced. The *intensity* measured by LIDAR is actually the power intercepted by the aperture of the LIDAR. The solid angle that this represents falls off with distance

This effect is important because it means that the relative distances to the sources of returns has a large effect on their relative intensities.

As shown in Figure 3 light hitting glass at an angle θ will be both transmitted and reflected at the same angle on the opposite side of the normal. Typically, about 8% of the light is reflected and the rest transmitted. Because of dust and microscopic imperfections in the surface of the glass, some of the light is scattered to nearby angles.

A quantitative discussion of the scattering physics of glass is beyond the scope of this paper, but notice that when θ is

[1] Some scanners, such as Hokuyo URG models, also use phase shift mechanisms [7] which are more affected by background objects, but the physics is similar.

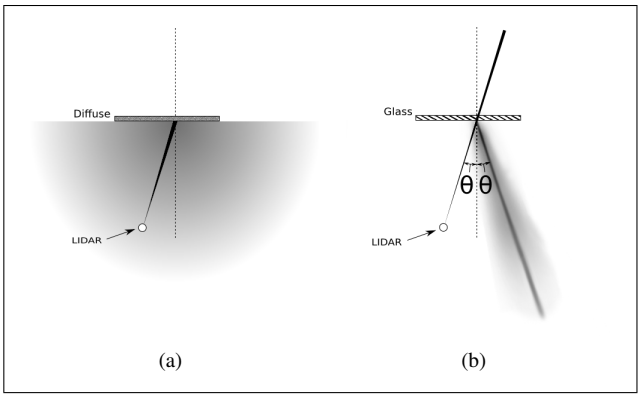

Fig. 3. Light behaves very differently when it hits different materials. Traditional LIDAR mapping algorithms assume that all surfaces are diffuse, as in (a), meaning they scatter incoming light equally in all directions. Light hitting glass however, as in (b), is split into three components. About 92% is transmitted through the glass; 8% reflects back at an angle opposite the incident angle, forming the *specular* reflection; and a very small percentage is scattered to angles near the specular direction by surface imperfections and dust. The glass therefore tends only to be detected when the laser ray strikes the surface at a near perpendicular angle. The effect is similar for mirrors and other shiny surfaces, except that they tend to lack the transmitted component.

near 0, the intensity of the return from the glass is much brighter than the intensity of the return from a diffuse object at the same distance.

2) LIDAR and Multiple Returns: Many LIDARs used in mobile robotics are designed to return only one distance reading per sample. In the case where light from more than one object is returned at the same time, the LIDAR must choose what range to report. For ranging purposes, it is more useful to read a range that corresponds to one of the returns than an averaged return. Therefore manufacturers go to some trouble to produce devices that distinguish the returns and choose one of the ranges to report [7], [8].

The methods that a LIDAR uses to distinguish multiple returns are fairly complex [9], [10]. In both time of flight and phase shift based LIDARs, the reported range is a function of the amount of light in each return and the range of each return. However for any fixed difference of ranges, increasing the light of a return tends to make it dominate the reported range reading [9],[11]. Because the intensity of the return from the glass changes suddenly with angle, the return from glass quickly goes from having little effect on the range reading to completely dominating the reading. For our purposes, a good working approximation to the LIDAR's behavior is that the range reading is not of the *closest* reflection, but of the *brightest* reflection.

Consider the case in Figure 4 where there is a diffuse wall behind a glass wall. The intensity of the returns for each is shown schematically as a function of angle in Figure 5. When the LIDAR is at a near normal angle to the glass, the return will be greater from the glass, and so the range to the glass will be read. At wider angles, the range to the diffuse wall will be read. There is some critical angle between the two where the returns are of equal intensity. Due to noise in the measurement, there is also a small range of angles near the

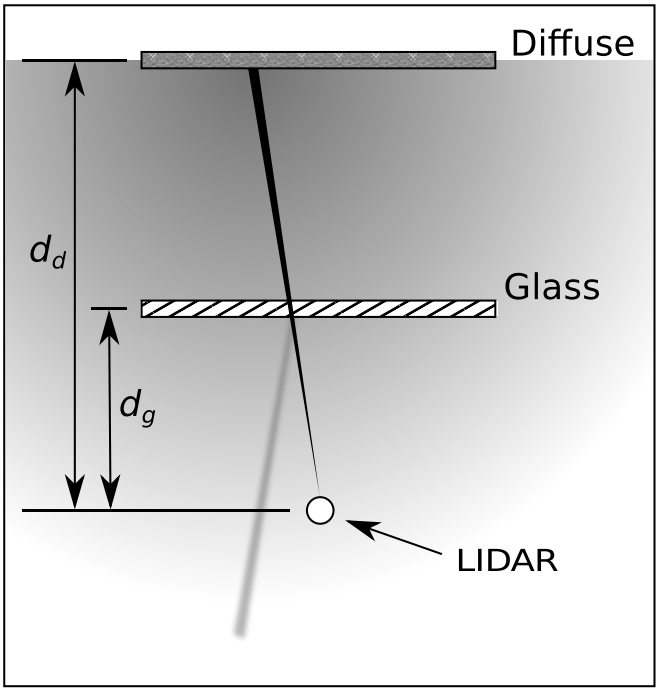

Fig. 4. When a diffuse wall is behind a piece of glass the returned light is a mixture from both. The received return intensities vary with angle and distance (See Figure 5).

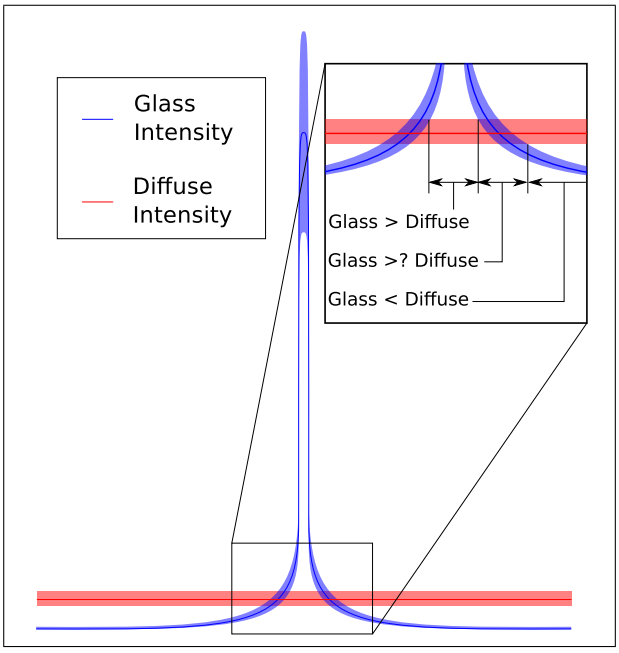

Fig. 5. When a diffuse wall is behind a piece of glass, as in Figure 4, the light returned to the LIDAR is made of a component from the diffuse wall(red) and the glass (blue), with some random variation (lighter areas). Because the LIDAR uses the light of the brightest return there are distinct ranges of angles where only the glass is detected or the diffuse wall. These are separated by a small range where the choice is indeterminate.

critical angle where either return may be selected.

The exact value of the critical angle is sensitive to the distance between the glass and the diffuse wall, and the distribution of dust on the glass. In complicated real world environments, with smudged glass and cluttered backgrounds, it is very difficult to predict the critical angle. There may even be multiple regions where the glass is visible.

Despite all of the uncertainty, the angles where glass is visible are fixed given a static background. Also, the glass is always visible when seen from directly normal to its surface. Our algorithm exploits this fact to find the angles where glass is reliably visible, and builds up an occupancy grid using the observations within those angles.

B. Sensor and World Models

1) World Model: We model the world as a grid of cells. Each cell may be occupied by a static object or a dynamic object, or may be empty. A dynamic object may appear in an empty cell or leave a cell it previously occupied. Each occupied cell has a *visibility function*, $\mathrm{VIS}(\phi)$, which is the probability, as a function of view angle[2], ϕ , that the return from that cell will be brighter than all farther[3] cells.

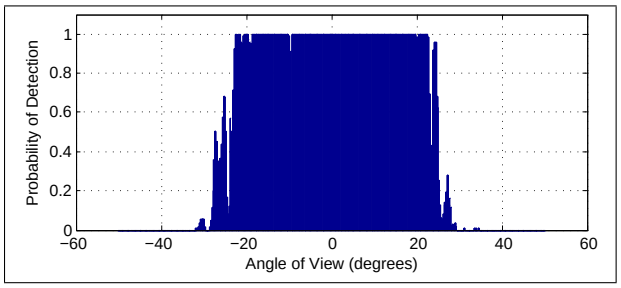

Fig. 6. With no objects behind the glass, it is visible to the lidar from a very wide range of angles. For any given angle, the probability of detection tends to be very close to 1 or 0. We call this probability the visibility function. For an ideal diffuse object the visibility function is always 1, so we refer to the range of angles where the visibility function is close to 1 as diffuse-like angles. (0.25° bins shown, d_g=1 m, d_d >20 m)

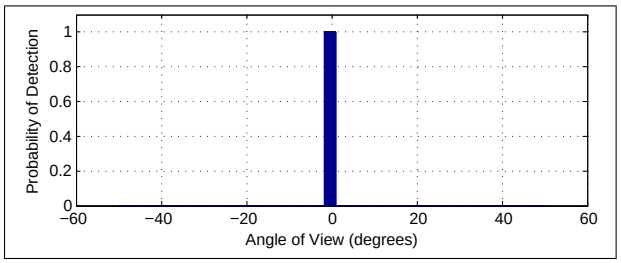

Fig. 7. The visibility function for the same glass as in Figure 6 with a diffuse wall 1 m behind. The glass is now visible from only a small range of angles, corresponding to the central peak in Figure 5 (0.25° bins shown,d_g=1 m, d_d=2 m)

An example of this function taken from a point on a piece of glass is shown in Figure 6. It the following figure, the visibility function for the same glass with a wall 1 m behind it is shown. As predicted by the theory above, the visibility is composed of blocks of angles where the probability of detection is nearly 1 separated by the critical angles, where the probability is intermediate, from angles with probability near 0. Even in the unusually bad case of a diffuse wall directly behind the glass, there is still a reliable set of angles from which the glass is detectable.

We assume the prior probability of a cell containing a static obstacle is a small value, and it is therefore safe to assume that a cell is empty, in the absence of other knowledge, in accordance with the observation that surfaces typically make up a small fraction of the cells in the environment.

2) Sensor Model: In our model, the LIDAR shoots a laser into the environment with angle ϕ. The laser returns from the first surface with a probability $\mathrm{VIS}_1(\phi)$, from the second surface with a probability $(1 - \mathrm{VIS}_1(\phi)) \cdot \mathrm{VIS}_2(\phi)$, and so on. Thus, the probability of observing a return from surface n, an event which we denote Z_n, can be written as

$$p(Z_n) = VIS_n \cdot \prod_{i=0}^{n-1} (1 - VIS_i) \tag{1}$$

Aside from the process of selecting the brightest return, the behavior of the LIDAR is considered the same as for the diffuse single return case. We assume gaussian distributed range error, and have small probability, p_{rand} ($\approx 1 \times 10^{-3}$ for our LIDAR), that the LIDAR will fail and produce a random reading[4].

This is nearly identical to the normal sensor model, except that the standard model assumes that $\mathrm{VIS} \approx 1$ at all angles. Therefore, if it is possible to discover the ranges of angles where $\mathrm{VIS}(\phi) \approx 1$ and only use measurements taken from those angles, then standard occupancy grid methods can be used for mapping glass. We refer to these angles as the diffuse-like view angles for each cell.

IV. VISAGGE

The core of our algorithm consists of a standard occupancy grid which is only updated when viewing objects from known diffuse-like angles. To this is added a second layer where we store a range of diffuse-like angles for each cell. In order to provide high confidence updates to the occupancy grid, we use an algorithm to check that we have actually passed through a diffuse-like angle before updating, which requires a third layer where we store recent angles of view relative to each cell. Finally, we use a heuristic to improve motion detection when traversing the environment for the first time.

In deriving our algorithm we start with a static world assumption, which will be corrected in Section IV-B. To simplify discussion, we also assume the size of a cell is significantly larger than the error in the range or localization, and that localization information is already given, although

[2]The incidence angle (Figure 3(b)) $\theta = \phi - \phi_N$ where ϕ is the view angle (in a world centered frame) and ϕ_N is the (unknown but fixed) surface normal in the same frame.

[3]In this sense *farther* means optically farther, i.e. all reflections of other objects in a mirror are farther than the mirror.

[4]Many implementations artificially inflate p_{rand} in order to cause motion to wash out as sensor noise. Because glass can appear identical to a moving object, we must deal with motion explicitly to distinguish it from glass.

it is relatively straightforward to adapt our algorithm to situations where this is not the case.

A. Static world approximation

Occupancy grids work by accumulating nominally independent evidence for the competing hypotheses that a cell is occupied or empty [1].

The evidence for the hypothesis that a cell is occupied is simple: when an observation lands in that cell, it is more likely to be occupied. This is true for all materials.

The problem lies in determining evidence that a cell is not occupied. Recall that the standard occupancy grid assumes that VIS ≈ 1 for all surfaces. This would imply that (1) becomes:

$$p(Z_n) \approx \begin{cases} 1, & \text{if } n = 1 \\ 0, & \text{otherwise} \end{cases} \tag{2}$$

assuming that there is at least one obstacle in the path of the laser.

In other words, observing a cell makes it very likely that the cell contains the closest obstacle along the path of the laser. Conversely, it is unlikely the laser would get that far if there were any closer surfaces.

In the presence of glass, the situation is entirely different. For glass, $\mathrm{VIS}(\phi) \approx 0$ at most angles, so any observations beyond the glass tend to give very little information on whether the glass is actually present.

One possible solution to this problem is simply to never count any observation as evidence against a cell being occupied. This amounts to never freeing a cell once it is occupied. In a truly static world, this works surprisingly well because p_{rand} is so low. As long as the sensor is not stationary for a long time, random errors will not accumulate in any given part of the map.

B. Detecting motion in multiple passes

Unfortunately for this mapping approach, the world is rarely completely static. It is essential to have a method for detecting that cells are no longer occupied. We solve this by noting that observations of static objects are highly repeatable because $\mathrm{VIS}(\phi)$ usually only takes on values close to 1 or 0.

In Figure 8 we show that if a static object at point P is observed from a known diffuse-like angle then it is sure to be re-observed when passing through the same angle again, even taking into account localization and range error.

What if we don't observe anything at P? This would imply that one of our assumptions is wrong. Either the LIDAR is in error, or the object has moved.

Recall that the LIDAR very rarely produces false negatives. This means that the most likely explanation is that the object at P has moved, and that the cells it occupied are now empty. If we consider our occupancy grid as storing the log odds likelihood that a cell is occupied (the "occupancy"), then this is equivalent to saying that we should decrement the occupancy of cells near P. If we decide that the object in the cell really has moved, we should discard any knowledge we have about $\mathrm{VIS}(\phi)$ for that cell, since presumably the visibility function for whatever might be in the cell now is unrelated to whatever was in it before.

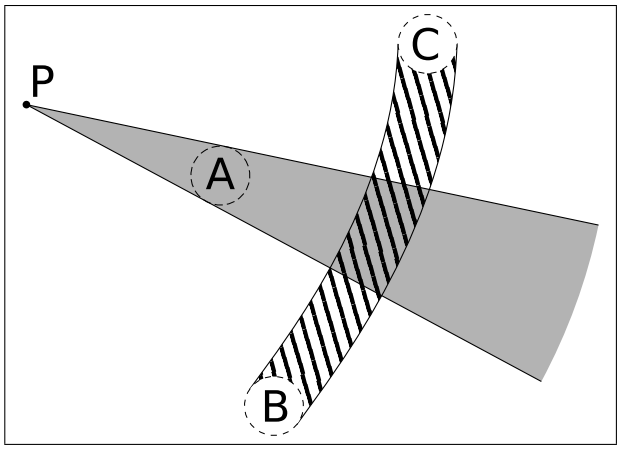

Fig. 8. Suppose that an object exists at point P, that we have observed this object from A, and by means of some external information we know that $\mathrm{VIS}(\phi) = 1$ for whatever ϕ we were observing from. In other words, we observed it from a diffuse-like angle. Due to localization and range error, we may actually have observed P from anywhere within the circle around A. This means that somewhere in the shaded region is a line of sight to P. If at some later time we travel from B to C, and, taking uncertainty into account, we know that our path from B to C must have passed through the cross hatched region. Then, assuming the LIDAR has not made a mistake, and the object is static, *we are certain to re-observe the object at P from somewhere along our path.*

Why this relatively complicated mechanism for showing that a cell is empty? By using the probability distribution for the position of A, we could work out a probability distribution for the line of sight, and then estimate our chance of seeing the object at P again, at any given time. Then the lack of observations along our path would provide evidence against P being in the same location as before.

The problem with simply using the probabilities at each time step is that it assumes the observations (or lack thereof) are independent. At every moment the best we can do is say that we *probably* should have seen the object if our assumptions are correct. With the proposed method we know when we *almost certainly* should have seen the object. In other words, the proposed method significantly increases the strength of the evidence against the hypothesis that the cell still contains the object. This increases the rate of convergence for our algorithm.

As an example, consider the case where the object at P is visible from only a single angle and that angle is equally likely to be anywhere in the shaded region. We would then have a 50% probability of seeing the object when passing through the first half of the shaded region, and 50% probability of seeing it when passing through the second half. If we treat these two events as independent, then we would say that when passing through the entire region the chance of not seeing the object, given that it is static, is 25%. However, the real probability of not seeing the object is 0%. In other words, we should be absolutely certain that the object has moved (neglecting the possibility of unexpectedly

large LIDAR or localization error).

For glass, the range of angles where $\mathrm{VIS}(\phi) \approx 1$ is very small, 2° in the case shown in Figure 7. This means the expected number of observations in a single pass by the glass is very small. It is therefore desirable to have a very high confidence method for detecting that cells are unoccupied, to make the best use of what little information is available.

Notice that this repeatability argument works equally well for diffuse objects. In fact our algorithm uses exactly the same procedure for all materials. This allows our method to deal with all materials on the continuum from diffuse to specular or transparent, relying only on the fact that the material has at least some diffuse-like angles.

1) Determining diffuse-like angles: To use the preceding argument, we need a way to determine that $\mathrm{VIS}(\phi) \approx 1$. The most accurate method would be simply to traverse the environment repeatedly to sample $\mathrm{VIS}(\phi)$. However, this is impractical both because of the number of passes needed and the amount of memory needed to store $\mathrm{VIS}(\phi)$ to a sufficient resolution. A heuristic is necessary to approximate $\mathrm{VIS}(\phi)$ in a single pass. Awais [3] assumed that $\mathrm{VIS}(\phi)$ was a gaussian which significantly reduced the complexity of the problem, but as shown in Figure 6, $\mathrm{VIS}(\phi)$ is not even close to gaussian, leading to poor results.

As noted earlier, $\mathrm{VIS}(\phi)$ tends to be made up of blocks of angles where $\mathrm{VIS}(\phi) \approx 1$ or $\mathrm{VIS}(\phi) \approx 0$. This means that any given observation tends to correspond to a place where $\mathrm{VIS}(\phi) \approx 1$. Also, because $\mathrm{VIS}(\phi)$ has a blocky distribution, and the centers of blocks are closer to 1, a contiguous string of observations tends to contain many angles where $\mathrm{VIS}(\phi) \approx 1$.

A simple way to take advantage of this structure is to record the widest range of angles from which the cell has been continuously observed.

This heuristic is also convenient in that it is easy to update online by keeping track of the range of angles in the current run of observations, and replace the previous best whenever it is exceeded by the current range.

In a similar fashion, it is easy to keep track of the range of angles traversed by the sensor since the cell was last observed or occluded. These angles sweep out a sector that can be used as the crosshatched region in Figure 8.

2) Determining occlusion: The above implicitly assumes that the object at P is not occluded. If a cell is occluded, then no information can be gained about that cell because the laser didn't reach it. In other words we should not alter the cell's occupancy if it is occluded.

Usually, when a cell is occluded, the LIDAR returns the range of the occluding object. We are not aware of any process by which the LIDAR produces a range reading closer than the closest object. Thus, if the range reading was closer than P , then the cell was definitely occluded and we gain no information.

A cell may also be occluded if an object such as a mirror or glass reflects the laser to some other object, producing an anomalously long range reading. If we have already mapped the offending surface, we can check for this as well and prevent readings that pass through the surface from affecting further cells.

3) Summary: Our main algorithm algorithm is as follows:

VISAGGE CORE

1: When an observation lands in a cell, increment its occupancy.
2: For every cell, record the widest range of angles (relative to the cell) from which the cell was continuously observed. Call this range ϕ_{VIS}.
3: For every cell, keep track of the angular range traversed by the LIDAR since the cell was last observed or occluded. Call this range ϕ_{MISS}.
4: When ϕ_{MISS} overlaps ϕ_{VIS} by more than can be explained by localization uncertainty, decrement the occupancy.
5: When a cell's occupancy drops low enough that it is probably free, delete ϕ_{VIS}.

C. Detecting motion in a single pass

It is always possible for an object to move in such a way as to simulate the pattern of observations hitting a piece of glass. However, in the case of multiple passes, the pattern of observations on glass repeats in concert with the motion of the sensor. This is unlikely for a moving object unless the object's motion is dependent on the motion of the sensor. Because the algorithm discussed so far works by eliminating points that are not repeatably observed it requires two passes to distinguish motion from glass.

Nevertheless, in many situations, such as a robot initially exploring an unknown environment, the sensor only traverses the environment once. In this case, the sensor is quite likely to pass through any given range of view angles only once, so it is desirable to produce a correct map of the environment after a single pass. We also note that when considering a single point seen from only a single pass, glass is indistinguishable from an object in motion. This is because at any given cell, a moving object manifests itself as an isolated period of time when the cell is observed, which is precisely how glass appears.

It is possible, however, to distinguish glass based on non-local information. The reason that we can detect glass at all is that light is reflected back when it hits the surface at a normal angle. This means that the diffuse-like angles of the surface definitely includes the normal to the surface. Similarly, the range of diffuse-like angles for all surfaces in a region of space is a superset of the range of surface normals in that region of space. So, if we pass a region of space and only observe cells in that region from a very narrow angular range, the surfaces in that region must have a very small range of normals, assuming the surfaces are stationary. This means that we know the surfaces in that region of space must be both very flat and fall within a small range of orientations. Such a surface will very likely extend into neighboring cells in both directions perpendicular to the normal direction.

A cell containing a moving surface also tends to have a small number of observations coming from a single direction, corresponding to the direction to the sensor at the time the moving moving surface happened to be in that cell. However, there are no constraints on how the neighboring cells are occupied.

We distinguish these two cases by a heuristic for separating motion after a single pass:

SINGLE PASS MOTION REMOVAL

1: Select the cells whose ϕ_{VIS} have a low width ($< 6°$ in our implementation). Mark these cells as uncertain.
2: Find any uncertain cells that don't have occupied or uncertain neighbors on both sides normal to the direction of observation (the mean of ϕ_{VIS}). Mark those cells as unoccupied.
3: Repeat 2 until convergence.

This heuristic is less reliable in the long run than the core algorithm because it does not eliminate motion that consistently travels perpendicular to the line of sight from the LIDAR to the object, such as a pedestrian walking side by side with the LIDAR at a fixed distance, or a self reflection when moving parallel to a piece of glass or mirror. The heuristic may also eliminate glass that has a small diffuse surface behind it (as is the case with the pillars in Figure 2(c)), because in these cases we may select a ϕ_{VIS} that doesn't include the normal. Because of this, we recommend not using this heuristic when two or more passes have been made by a cell.

V. EXPERIMENTS AND RESULTS

In order to evaluate our algorithm, and the sensor model it is based on, we ran two experiments using a Hokuyo UTM-30LX LIDAR with intensity reporting information producing scans at 40Hz.

A. Validation of sensor model

We evaluated our sensor model by comparing intensity readings from diffuse and non-diffuse surfaces.

As shown in Figure 9, the intensity readings closely parallel the theoretical shapes shown in Figure 5. In addition, the intensity of the diffuse surface falls away with distance. From Figure 9, it can be seen that the glass is brighter than the diffuse wall for an incidence angle of $\pm 1°$ when both are at about the same distance. This would imply that the glass should be visible in a $2°$ wide range, as was indeed observed in Figure 7. Similarly, when there is nothing behind the glass, it should be visible for a wide but more variable angle due to the noise at low intensity, as was observed in Figure 6.

B. Mapping

We evaluated the actual mapping performance of our algorithm by driving a LIDAR equipped wheelchair through the environment shown in Figure 1. We drove at approximately 1 m/s in a single pass around the walkway, which covers a

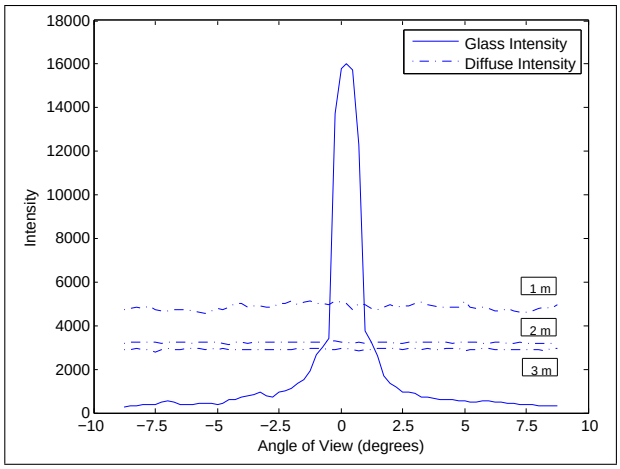

Fig. 9. Our sensor model assumes that the brightest return is used to compute the range reading for the LIDAR. To test this, we measured the intensity reported by a Hokuyo UTM-30LX (*not* linear with true intensity) from the glass and diffuse surfaces in Figures 6 and 7. As expected, the intensity varied mainly as a function of distance for a diffuse surface, and mainly by angle for glass (for readability, 1 m shown only). With the diffuse surface at 2 m, the glass is brighter over a range of approximately 2°. This closely parallels the range in which the glass was detected in Figure 7, validating the theory.

20 m x 20 m floor space, as shown in Figure 2. The walkway is entirely enclosed by glass on its inner wall. We ran our algorithm in an online manner (i.e. incrementally) on a previously collected dataset with precomputed sensor localization information [5] with the single pass motion removal included. The algorithm averaged 9.1 ms/scan running on a 2.0 GHz Intel® Core™2 CPU. We also ran a standard occupancy grid algorithm on the same data for comparison.

The results are displayed graphically in Figure 2.

As shown in Figure 10 our algorithm performs significantly better than the traditional occupancy grid mapping method on glass walls, correctly detecting 95% of the glass, as compared to 13% for the traditional method.

We also noted that our algorithm correctly detected the stainless steel surface of the elevator, seen at the top of Figure 2(b), validating our assumption that our algorithm works on partially specular materials.

As expected from the discussion in Section IV-C, our algorithm intermittently failed to detect glass when an isolated object (usually a pillar) was directly behind the glass. Qualitatively, this is not a particularly bad failure mode for a mobile robotics application since the nearby object would prevent a path planner from trying to plan paths through the missing section.

The performance of our algorithm in terms of false positives is similar to the traditional occupancy grid, with somewhat more errors in rejecting reflections, due largely to reflections of the wheelchair moving parallel to the glass,

[5] Both MATLAB and C++ implementations without single pass motion removal are available at `http://irlab.eecs.umich.edu/website/dataset/Glass_wall_icra2013.html` as well as the datasets used. Single pass motion removal is withheld because our implementation used modified versions of internal MATLAB functions. We are working to provide a free version of this code.

		Traditional Grid Mapping		VisAGGE	
Glass	Correctly Detected	13.29%	99	94.90%	707
	Incorrectly Localized	1.21%	9	0.94%	7
	Total Ground Truth	745			
Motion	False Positive	1.09%	43	0.35%	14
	Total Ground Truth	3954			
Reflection	False Positive	2.24%	61	5.17%	141
	Total Ground Truth	2727			

Fig. 10. The performance of our algorithm (VisAGGE) and the standard occupancy grid algorithm were measured by comparing with a ground truth generated by hand labeling each cell observed as glass, diffuse, motion, or reflection (Figure 2(b)). Diffuse cells were excluded from further analysis. The values in the table were derived as follows:
The walls from the algorithms' outputs and the ground truth were thinned before comparison to determine localization accuracy, and to measure total glass length. Glass cells on the ground truth were considered correctly detected if they were within one cell of an occupied cell in the output, and detected but incorrectly localized if they .
The un-thinned versions of the maps were used to determine false positives. Any cells reported as occupied and coincident with cells marked as motion or reflections in the ground truth were considered false positives.
Finally, in the top right corner of the map there was a set of chairs with seats at precisely the same height as the LIDAR plane, causing "flickering" detection, making it unclear whether they should have been detected as motion or not. These cells were ignored in the analysis.

and somewhat fewer errors caused by moving objects, due to having a more sensitive motion detection scheme.

A separate qualitative[6] evaluation was done with a mirrored wall. Our algorithm showed slightly faster detection and less noise with the mirror than the glass, presumably because more light was reflected back, but was generally quite similar to glass. We emphasize that the algorithm was not modified in any way to deal with the mirror.

VI. CONCLUSION

In this paper we have detailed an online algorithm for performing occupancy grid mapping in the presence of glass and other non-diffuse surfaces.

Our method is based on a sensor model which allows the problem of mapping glass to be converted into a standard occupancy grid mapping problem given knowledge of a set of of angles from which glass appears like a diffuse surface. We have given a heuristic for determining a subset of these diffuse-like angles and a method for generating high confidence inferences from observations at these angles. We have also given a heuristic to improve discrimination between motion and glass in cases where the environment has only been traversed once.

Experimental investigation of the behavior of our LIDAR has shown good agreement with the predictions of our sensor model. We have shown experimentally that this algorithm is robust to motion and can be used to build a map of the environment in a single traversal, with quality comparable to a standard occupancy grid on diffuse surfaces while simultaneously providing good detection and localization of both flat and curved glass surfaces. In the future we hope to implement our algorithm in a realtime mobile robotics environment and evaluate its performance on a wider range of materials.

[6]Due to having only 1m of mirrored wall, equating to only 20 cells in our map. Dataset is available from the website.

REFERENCES

[1] S. Thrun, W. Burgard, and D. Fox, *Probabilistic Robotics*. Cambridge, MA: MIT Press, 2006.

[2] A. Diosi and L. Kleeman, "Advanced sonar and laser range finder fusion for simultaneous localization and mapping," in *IEEE/RSJ International Conference on Intelligent Robots and Systems (IROS), 2004. Proceedings. 2004*, vol. 2. IEEE, 2004, pp. 1854–1859.

[3] M. Awais, "Improved Laser-based Navigation for Mobile Robots," in *International Conference on Advanced Robotics (ICAR), 2009.* IEEE, 2009, pp. 1–6.

[4] S. Yang and C. Wang, "Dealing with Laser Scanner Failure: Mirrors and Windows," in *IEEE International Conference on Robotics and Automation (ICRA), 2008.* IEEE, 2008, pp. 3009–3015.

[5] S. Pu and G. Vosselman, "Knowledge based reconstruction of building models from terrestrial laser scanning data," *ISPRS Journal of Photogrammetry and Remote Sensing*, vol. 64, no. 6, pp. 575 – 584, 2009. [Online]. Available: http://www.sciencedirect.com/science/article/pii/S0924271609000501

[6] A. Tatoglu and K. Pochiraju, "Point Cloud Segmentation with LIDAR Reflection Intensity Behavior," in *IEEE International Conference on Robotics and Automation (ICRA), 2012.*, May 2012, pp. 786 –790.

[7] H. Kawata, K. Miyachi, Y. Hara, A. Ohya, and S. Yuta, "A Method for Estimation of Lightness of Objects with Intensity Data from SOKUIKI Sensor," in *IEEE International Conference on Multisensor Fusion and Integration for Intelligent Systems (MFI), 2008.* IEEE, 2008, pp. 661–664.

[8] C. Ye and J. Borenstein, "A new terrain mapping method for mobile robots obstacle negotiation," in *UGV Technology Conference at the 2003 SPIE AeroSense Symposium*. Citeseer, 2003, pp. 21–25.

[9] M. Adams and P. Probert, "The Interpretation of Phase and Intensity Data from AMCW Light Detection Sensors for Reliable Ranging," *The International Journal of Robotics Research*, vol. 15, no. 5, pp. 441–458, 1996. [Online]. Available: http://ijr.sagepub.com/content/15/5/441.abstract

[10] J. Tuley, N. Vandapel, and M. Hebert, "Analysis and Removal of Artifacts in 3-D LADAR Data," in *IEEE International Conference on Robotics and Automation (ICRA), 2005.*, april 2005, pp. 2203 – 2210.

[11] C. Ye, "Mixed Pixels Removal of a Laser Rangefinder for Mobile Robot 3-D Terrain Mapping," in *International Conference on Information and Automation(ICIA), 2008.* IEEE, 2008, pp. 1153–1158.